

# THRESHOLD GRAPHS ARE GLOBALLY SYNCHRONIZING

HONGJIN WU AND ULRIK BRANDES

ABSTRACT. The Kuramoto model can be formulated as a gradient flow on a nonconvex energy landscape of the form  $E(\boldsymbol{\theta}) := \frac{1}{2} \sum_{1 \leq i, j \leq n} A_{ij} (1 - \cos(\theta_i - \theta_j))$ . A fundamental question is to identify graph structures for which this landscape is benign, in the sense that every second-order stationary point corresponds to a fully synchronized state. This property guarantees that all trajectories of the Kuramoto model converge to a fully synchronized state except for a measure-zero set of initial conditions, a phenomenon known as global synchronization. Existing guarantees typically require that each node be connected to a sufficiently large fraction of the other nodes, enforcing high graph density. In this work, we show that threshold graphs lie well outside this regime while still exhibiting global synchronization. In particular, threshold graphs realize arbitrary edge densities and have degree sequences that are extremal in the sense of majorization. Our analysis is based on a phasor–geometric characterization of stationary points that exploits the structural and geometric symmetries induced by threshold graphs.

## CONTENTS

1. Introduction	2
1.1. Problem Setting	3
1.2. Nonconvex Optimization Landscape	4
1.3. Prior Work	4
1.4. Our Contribution	5
1.5. Structure of the paper	6
1.6. Notation	6
2. Preliminaries of Threshold Graphs	6
2.1. Definition and Characterizations	6
3. Preliminaries on the Kuramoto Model	7
3.1. Equilibria and Local Stability	7
3.2. Stationary Points and Local Optimality	8
3.3. Correspondence Between the Two Sets of Concepts	8
4. Vector Geometry of Equilibria	9
4.1. Vector-labeled Graph	9
4.2. Alignment and Equilibrium	9
4.3. Angles and Second-Order Stationarity	11
5. Local Synchronization Primitives	12
5.1. A Fundamental Geometric Fact	12
5.2. Phasor Geometry of Closed Twins	13
5.3. Synchronous Pendant Extension	15
6. Main Proof: the Induction Argument	18
6.1. A Prototype Example	18
6.2. Proof of Theorem 1.2: General Case	19
7. Discussion: Beyond Density-Based Guarantees	20
7.1. Threshold Graphs Realize All Densities	20
7.2. Degree Sequence of Threshold Graphs	20

*Date:* February 6, 2026.

8. Summary and Open Problems	21
Acknowledgements	21
References	21

## 1. INTRODUCTION

The study of synchronization traces back to the 17th century, when Christiaan Huygens first observed the spontaneous synchronization of pendulum clocks. Since then, synchronization phenomena have been widely studied across both natural and technological systems. For example, the flashing of fireflies [BB68, SS93], the rhythmic beating of heart cells [Win67, MS06], synchronization in power grids [DB12], coordinated motion in robotic networks [OS06], modern artificial intelligence models such as neural networks [MLGW24], and Transformer architecture [GLPR25, CRMB24].

A major obstacle in the study of synchronization was the absence of a model that simultaneously offered analytical tractability and sufficient dynamical richness. The Kuramoto model, introduced by Yoshiki Kuramoto in 1975 [Kur75], provided precisely such a balance, and has since become a central and widely accepted model for analyzing synchronization phenomena.

The Kuramoto model describes  $n$  oscillators on the unit circle, coupled according to a graph  $G = (V, E)$  with adjacency matrix  $A$ . Mathematically, it is a set of ordinary differential equations

$$\frac{d\theta_i}{dt} = \omega_i + \sum_{j=1}^n A_{ij} \sin(\theta_j - \theta_i), \quad i \in V,$$

where  $\theta_i : \mathbb{R} \rightarrow \mathbb{S}^1$  denotes the phase of oscillator  $i$ . Specifically, each oscillator is driven by its intrinsic frequency  $\omega_i$  and by the nonlinear interactions determined by the phase differences with its neighbors.

Early studies of the Kuramoto model primarily considered systems of oscillators with heterogeneous intrinsic frequencies  $\{\omega_i\}_{i=1}^n$ , coupled through a complete graph with uniform weights  $A_{ij} = K/n$ . Here,  $K$  denotes the strength of the coupling between oscillators. A fundamental question in this setting is to determine the critical coupling strength  $K_c$ , such that for  $K > K_c$ , the oscillators converge to a common frequency, a phenomenon known as *frequency synchronization*<sup>1</sup>, and for  $K < K_c$ , they remain desynchronized. This problem is of central interest across many scientific domains, ranging from biological synchronization, rhythmic phenomena [MMJ87], technological applications such as deep brain stimulation [NM11] and power systems [CCC95, DB12]. For comprehensive surveys of this line of work and its applications, we refer to [Str00, ABPV<sup>+</sup>05, DB14].

Another line of research focuses on the homogeneous Kuramoto model where all intrinsic frequencies are identical, i.e.,  $\omega_i = \omega$  for all  $i \in \{1, \dots, n\}$ . In this case, frequency synchronization is always achieved. This becomes immediate after applying a co-rotating frame  $\theta_i(t) \leftarrow \theta_i(t) - \omega t$ , under which the dynamics reduce to the gradient system

$$\frac{d\theta_i}{dt} = \sum_{j=1}^n A_{ij} \sin(\theta_j - \theta_i), \quad i \in V. \quad (1)$$

By LaSalle's invariance principle, every trajectory converges to the invariant set of equilibria satisfying  $\dot{\theta}_i = 0$  for all  $i$ . Thus, in the co-rotating frame, the asymptotic frequency of every oscillator is zero. Transforming back to the original coordinates, this implies that the oscillators always achieve frequency synchronization. In contrast, when intrinsic frequencies are non-identical, the dynamics may exhibit significantly more complex long-term behavior, including chaotic attractors [MPT05].

In the homogeneous setting, the remaining challenge is to determine whether *phase synchronization* occurs. This clearly depends on the initial conditions. If all oscillators start within a

---

<sup>1</sup>That is, all derivatives  $\frac{d\theta_i(t)}{dt}$  become identical as  $t \rightarrow \infty$ .

half circle, they converge to a common phase. However, beyond the half-circle region, the global behavior remained poorly understood for a long time.

Over the past two decades, a central question that has emerged is the following: under what graph structures does the homogeneous Kuramoto system achieve phase synchronization for all initial conditions, except for a set of measure zero? This problem is not only mathematically appealing but also closely connected to several recent developments across different research areas, including the Burer–Monteiro approach for semidefinite programming [BBV16, LXB19, Lin25] and the dynamics of Transformer architectures [GLPR25, GLPR23].

In this work, we follow this line of research, and beginning with a precise formulation of the problem.

### 1.1. Problem Setting.

**Definition 1.1** (Globally synchronizing graph). We say that a graph  $G = (V, E)$  is *globally synchronizing* if, for all initial conditions  $\boldsymbol{\theta}(0) \in \mathbb{R}^n$ , except for a set of measure zero, the solution to the Kuramoto model (1) on  $G$  satisfies

$$\lim_{t \rightarrow \infty} (\theta_i(t) - \theta_j(t)) = 0 \quad \text{for all } i, j \in V.$$

This naturally raises the following question:

**Key question.** *Which graphs are globally synchronizing?*

To build some intuition for the model (1) and the definition (1.1), one may imagine placing  $n$  oscillators on the unit circle and connecting them by edges specified by the adjacency matrix  $A$ . If there is an edge between nodes  $i$  and  $j$ , then whenever their phases differ, the interaction tends to reduce this difference and pull them toward a common phase.

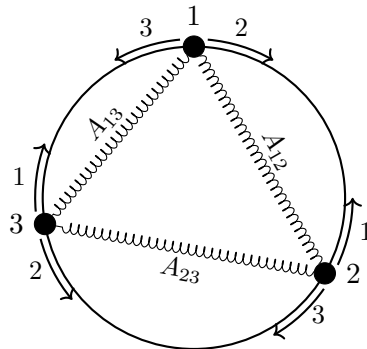


FIGURE 1. A spring analogy for a coupled oscillator network. The label on each curved arrow marks which node exerts the force.

From the above illustration of the complete graph  $K_3$ , one may ask whether the three oscillators will eventually converge to a common position when placed as shown in Figure 1. Each node is subject to two forces, for instance, node 1 is pulled toward node 2 on one side and toward node 3 on the other. So it is not immediately clear in which direction it will move, let alone whether all three nodes will ultimately coincide. Even in this simple example, the difficulty of the problem becomes apparent. Nevertheless, one may form an intuitive if somewhat heuristic expectation: since in a complete graph each oscillator tends to move closer to every other oscillator, the abundance of interactions may indeed drive the system to synchronize from almost all initial configurations.

**1.2. Nonconvex Optimization Landscape.** From an optimization viewpoint, global synchronization can be implied by the absence of spurious second-order stationary points of the nonconvex energy function. Precisely, the Kuramoto model (1) defines a *gradient dynamical system* (or called *gradient flow*<sup>2</sup>) with energy function  $E_G(\boldsymbol{\theta})$ , satisfying

$$\frac{d\boldsymbol{\theta}}{dt} = -\nabla E_G(\boldsymbol{\theta})$$

where  $E_G(\boldsymbol{\theta}) : (\mathbb{S}^1)^{|V|} \rightarrow \mathbb{R}$  with graph  $G = (V, E)$  is defined as

$$\begin{aligned} E_G(\boldsymbol{\theta}) &:= \frac{1}{2} \sum_{1 \leq i, j \leq n} \mathbf{A}_{ij} (1 - \cos(\theta_i - \theta_j)) \\ &= \frac{1}{2} \sum_{1 \leq i, j \leq n} \mathbf{A}_{ij} (1 - \langle \mathbf{v}_i, \mathbf{v}_j \rangle). \end{aligned} \tag{2}$$

Here,  $\mathbf{v}_i$  is the unit vector  $(\cos \theta_i, \sin \theta_i) \in \mathbb{R}^2$ .

Clearly, this function is nonconvex. Moreover, understanding the geometry of (2) provides direct insight into the long-term dynamics of (1). In particular, the synchronous states correspond exactly to the global minima of this energy function, and those minima that are local but not global (called *spurious local minima*) correspond to non-synchronous stable equilibria. If such spurious local minima exist, the gradient dynamics may converge to them whenever the initialization lies within their basin of attraction, in which case the graph  $G$  is not globally synchronizing.

In contrast, if the energy function (2) admits no spurious second-order stationary points, in the sense that the only equilibria at which the Hessian  $\nabla^2 E_G(\boldsymbol{\theta})$  is positive semidefinite are the fully synchronized states, then the graph  $G$  is globally synchronizing. A rigorous proof of this statement can be established using the Łojasiewicz gradient inequality [Lag07] together with the center manifold theorem; see Lemma A.1 in [GLPR25] for an excellent exposition.

**1.3. Prior Work.** Previous works on globally synchronizing graphs primarily focus on identifying sufficient conditions that guarantee global synchronization. A dominant line of research formulates this question from an extremal combinatorics perspective:

**Problem 1.** Let  $\delta(G)$  denote the minimum degree of  $G$ . Find the smallest constant  $\mu_c \in [0, 1]$  such that as long as  $\delta(G) \geq \mu_c(n - 1)$ , the graph is globally synchronizing.

Several advances have been made in [Tay12, LXB19, LS20, KST21, Can22, YTT21]. The currently best known bounds on the critical minimum-degree threshold  $\mu_c$  satisfy  $0.6875 \leq \mu_c \leq 0.75$ , where the upper bound is established in [KST21], and the strongest known lower bound follows from [Can22]. It has been conjectured that the minimum-degree threshold for global synchronization is exactly  $\mu_c = 0.75$ , and that below this density, even highly connected graphs may fail to synchronize (see [TSS20] and Conjecture 5 in [BKMR25]).

Sufficiently large threshold for minimal degree enforces high density. Indeed, when  $\mu_c \geq 75\%$ , the total number of edges satisfies  $|E| \geq \frac{3}{8} n(n - 1)$ , which scales as  $O(n^2)$ . However, dense graphs do not necessarily global synchronize, as indicated by the examples in [TSS20]. How sparse a globally synchronizing graph can be? Townsend, Stillman, and Strogatz [TSS20] approached this problem by asking how few edges are required to transform a ring graph<sup>3</sup> into a globally synchronizing network. They showed that destabilizing all non-synchronizing twisted states requires adding  $O(n \log n)$  edges arranged in a specific manner, indicating that adding  $O(n \log n)$  edges to a ring graph in a strategic way may lead to global synchronization. Moreover, a line of work on global synchronization over

<sup>2</sup>We call a dynamical system a *gradient flow* on  $E(x)$  if it has the form  $\frac{dx(t)}{dt} = -\nabla E(x)$ . Its trajectories evolve along the steepest descent direction of  $E$ .

<sup>3</sup>A ring graph of size  $n \geq 5$  does not globally synchronize.

random graphs [LXB19, KST22, ABK<sup>+</sup>26, JMS25, McR25] provides further evidence that sparse networks can globally synchronize. A natural question is to determine the critical connectivity threshold for Erdős–Rényi graphs to exhibit global synchronization with high probability. The best known bound asserts that, for any  $\varepsilon > 0$ , global synchronization holds with high probability when  $p \geq (1 + \varepsilon) \frac{\log n}{n}$ , as shown in [ABK<sup>+</sup>26], with further refinements in [JMS25, McR25]. However, this regime still corresponds to graphs with  $O(n \log n)$  edges.

**1.4. Our Contribution.** In this work, we identify a class of graphs that admit global synchronization without requiring the minimum degree to exceed prescribed thresholds, and can have any edge density as will be shown in Section 7.

**Theorem 1.2.** *Any connected threshold graph globally synchronizes.*

Threshold graphs can be constructed starting from a single vertex by iteratively adding each new vertex as either: an isolated vertex connecting to no existing vertex, or a dominating vertex connecting to all existing vertices. This generative process is uniquely encoded by a binary sequence of length  $n - 1$ , where 0 denotes an isolated vertex and 1 a dominating one. See Figure 2 for examples. A full formal definition and additional characterizations are given in Section 2.

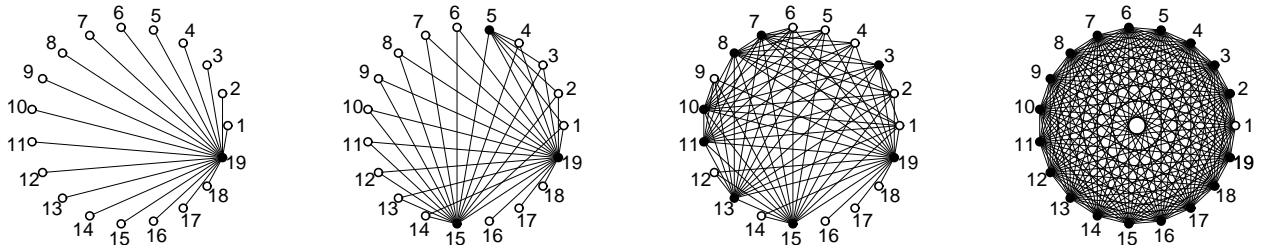


FIGURE 2. Four connected threshold graphs on 19 vertices, from the sparsest (star graph) to the densest (complete graph). Node labels indicate the vertex addition order in the construction, with vertex 1 as the initial vertex. White and black circles denote isolated and dominating vertices (bit 0 and bit 1), and the initial vertex 1 is colored in white. Codes from left to right: 00000000000000000001, 000100000000010001, 010001101101010001, 1111111111111111.

In terms of proving the main result, the difficulty arises from the fact that many existing proofs of global synchronization rely, either explicitly or implicitly, on the so-called *half-circle lemma*. This lemma states that if all oscillators are confined to an open half-circle, then the dynamics contract toward synchrony. Building on this observation, the bootstrap strategy seeks to show that all second-order stationary points must lie within a half-circle. If successful, this excludes the existence of non-synchronous states to which the dynamics may converge, thereby implying global synchronization.

However, for threshold graphs, it remains unclear how to apply this strategy. It typically depends on sufficient connectivity in the network thus naturally suited to dense graphs, where the large number of edges ensures that nodes inside the half-circle collectively exert sufficient force to pull outside nodes back into alignment. In contrast, threshold graphs span the full spectrum from extremely sparse examples, such as stars, to extremely dense ones, such as complete graphs, making it unclear how such techniques can be applied in this setting.

In this work, we bypass the half-circle approach by reducing the high-dimensional geometric question of whether the energy landscape is benign to a planar vector-geometric condition. This condition naturally leads us to study twins in the graph-theoretic sense, as well as a broader notion that we introduce, which we call *geometric twins*. The latter depends jointly on the graph structure and on the equilibrium configuration  $\boldsymbol{\theta}$ . These notions clarify how the relative positions of phases behave at second-order stationary point of the energy landscape  $E(\boldsymbol{\theta})$ . Building on this

understanding, we employ an inductive strategy: synchronization is first established locally on small substructures, and then shown to propagate across the whole graph along the neighborhood-inclusion hierarchy of threshold graphs.

*Understanding the Mechanism Behind Global Synchrony in Threshold Graphs.* Previous global synchronization results focus on density-based conditions. For instance, any graph whose minimum degree exceeds  $0.75(n - 1)$  is globally synchronizing [KST21]. In other words, these results require the graph to be sufficiently dense. Threshold graphs, however, lie outside this regime. Nevertheless, we prove in this work that they also exhibit global synchronization.

What deeper insight can we draw from this result? Our analysis shows that the global synchronization of threshold graphs is not a consequence of density. Instead, it arises from a different mechanism, namely the presence of local symmetries. Some of these symmetries come from the graph structure itself: as we show in Lemma 5.2, closed twins must synchronize at any second-order stationary point. There are also symmetries that do not originate purely from combinatorial structure, that is, certain configurations exhibit a form of geometric symmetry. As we will show in Section 5.3, in the configurations we call synchronous pendants, pairs of vertices that are not structurally symmetric nonetheless become geometrically equivalent at second-order stationary points and hence synchronize. Such symmetric configurations arise inductively along the construction process of threshold graphs. Their synchronization propagates backward from later-added vertices to earlier ones, which shows that every second-order stationary point is a synchronous state. Consequently, every threshold graph is globally synchronizing.

**1.5. Structure of the paper.** The preliminaries on threshold graphs and the Kuramoto model are presented in Sections 2 and 3, respectively. The basic geometric tools, referred to as *phasor geometry* or *vector geometry*, are introduced in Section 4. The key lemmas, termed *Local Synchronization Primitives*, which underpin our main proof, are presented in Section 5. The proof of the main result is given in Section 6. In Section 7, we discuss the density and degree sequence of threshold graphs. Finally, Section 8 concludes the paper with a discussion of open problems.

**1.6. Notation.** Throughout this work, all graphs are assumed to be connected and simple, i.e., without self-loops or weighted edges. We write  $u \sim v$  to indicate that vertices  $u$  and  $v$  are adjacent in a graph, and  $u \not\sim v$  otherwise. For a vertex  $i$  and a subset  $Q$  of vertices, we denote

$$N_Q(i) := \{q \in Q : q \sim i\},$$

the set of neighbors of  $i$  that lie in  $Q$ . We use  $\uplus$  to denote the disjoint union of sets.

We denote by  $\mathbb{S}^1 := \{\mathbf{x} \in \mathbb{R}^2 : \|\mathbf{x}\| = 1\}$  the unit circle. For vectors  $\mathbf{x}, \mathbf{y} \in \mathbb{R}^2$ , we write  $\mathbf{x} \uparrow \mathbf{y}$  to indicate that  $\mathbf{x}$  and  $\mathbf{y}$  are nonzero and positively collinear, i.e.,  $\mathbf{x} = \lambda \mathbf{y}$  for some  $\lambda > 0$ .

Following the convention in dynamical systems, we refer to the variable  $\boldsymbol{\theta} = (\theta_1, \dots, \theta_n)$  of the Kuramoto model (1.2) as the *state*, and call the solution  $\boldsymbol{\theta}(t)$  with initial condition  $\boldsymbol{\theta}(0)$  a *trajectory* starting from  $\boldsymbol{\theta}(0)$ .

## 2. PRELIMINARIES OF THRESHOLD GRAPHS

Threshold graphs are a well-studied class of graphs that play a central role in graph theory and have found applications across a wide range of disciplines. The term *threshold graph* was introduced by Chvátal and Hammer [CH77b] in their study of set-packing problems. Since then, threshold graphs have appeared in numerous settings, including resource allocation, cyclic scheduling, manpower planning, complexity theory, and the study of graphical degree sequences [CH77a].

### 2.1. Definition and Characterizations.

**Definition 2.1.** A graph  $G$  is called a *threshold graph* if it can be constructed from the one-vertex graph by repeatedly applying one of the following two operations:

- (i) add an *isolated* vertex, adjacent to no existing vertex;
- (ii) add a *dominating* vertex, adjacent to all existing vertices.

The resulting graph on vertices  $\{1, \dots, n\}$  is uniquely encoded by the binary sequence  $(b_2, \dots, b_n)$ , where  $b_i = 0$  if vertex  $i$  is added as isolated and  $b_i = 1$  if it is added as dominating node.

Although in this work we rely only on the construction process of threshold graphs to analyze their global synchronization, it is of independent interest to recall that they admit several equivalent characterizations [CH77b].

**Theorem 2.2.** *Let  $G = (V, E)$  be a graph. The following statements are equivalent:*

- (i)  $G$  is a threshold graph.
- (ii)  $G$  is obtained by iteratively adding isolated or dominating vertices to the one-vertex graph.
- (iii)  $G$  admits a weight function  $w : V \rightarrow \mathbb{R}$  and a threshold  $t \in \mathbb{R}$  such that

$$\{u, v\} \in E \iff w(u) + w(v) \geq t, \quad \forall u \neq v.$$

- (iv)  $G$  is  $\{P_4, C_4, 2K_2\}$ -free (see Fig. 3).
- (v) For any distinct  $u, v \in V$ ,  $N(u) \subseteq N[v]$  or  $N(v) \subseteq N[u]$ .

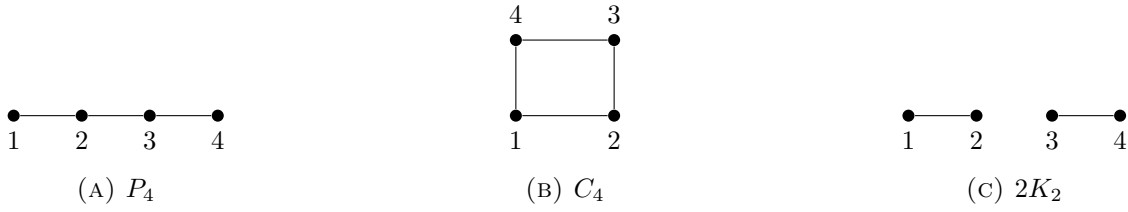


FIGURE 3. Forbidden induced subgraphs for threshold graphs.

**Remark 2.3.** Interestingly, threshold graphs appeared in the synchronization literature long before their role in the Kuramoto model was considered. In particular, as early as 1977, Ausiello, Messina, and Protasi [AMP77] introduced a class of graphs (later recognized as threshold graphs) in the study of synchronization primitives in distributed computation. Their work provided a graph-theoretic characterization of so-called  $PV_c$ -definable graphs, which encode combinatorial conditions under which simple local update rules lead to global agreement.

### 3. PRELIMINARIES ON THE KURAMOTO MODEL

**3.1. Equilibria and Local Stability.** By the definition, equilibrium points of a dynamical system are the states where the system remains at rest, meaning that the first-order derivative of the state vanishes [Kha02]. Thus setting the right-hand side of (1) to zero provides the characterization of an equilibrium point of the Kuramoto model.

**Definition 3.1** (Equilibria of (1)). We call  $\boldsymbol{\theta} \in \mathbb{R}^n$  an *equilibrium* of the Kuramoto model (1) if it satisfies

$$\sum_{j=1}^n \mathbf{A}_{ij} \sin(\theta_j - \theta_i) = 0, \quad \forall i \in [n]. \quad (3)$$

An equilibrium point is said to be stable if sufficiently small perturbations around it remain small for all future time [Kha02]. To assess the stability of a given equilibrium point, one typically studies the linearization of the system at that point, which is characterized by the Jacobian matrix.

**Proposition 3.2** (Stable equilibrium of (1)). *An equilibrium point  $\boldsymbol{\theta} \in \mathbb{R}^n$  of the Kuramoto model (1) is stable if the Jacobian matrix  $\mathbf{J}$ , defined as:*

$$\mathbf{J}_{ij} = \begin{cases} -\sum_{j=1}^n \mathbf{A}_{ij} \cos(\theta_i - \theta_j), & \text{if } i = j, \\ \mathbf{A}_{ij} \cos(\theta_i - \theta_j), & \text{if } i \neq j, \end{cases}$$

*is negative semi-definite.*

### 3.2. Stationary Points and Local Optimality.

**Definition 3.3** (First-order stationary points of (2)). *We call  $\boldsymbol{\theta} \in \mathbb{R}^n$  a *first-order stationary point* of the energy function (2) if it satisfies  $\nabla E(\boldsymbol{\theta}) = 0$ , namely*

$$\sum_{j=1}^n \mathbf{A}_{ij} \sin(\theta_j - \theta_i) = 0, \quad \forall i \in [n]. \quad (4)$$

**Proposition 3.4** (Hessian  $\mathbf{H}$  of (2)). *For the Kuramoto energy (2), the Hessian has entries*

$$\mathbf{H}_{ij} := (\nabla^2 E(\boldsymbol{\theta}))_{ij} = \begin{cases} \sum_{j=1}^n \mathbf{A}_{ij} \cos(\theta_i - \theta_j), & \text{if } i = j, \\ -\mathbf{A}_{ij} \cos(\theta_i - \theta_j), & \text{if } i \neq j, \end{cases}$$

**Definition 3.5** (Second-order stationary points of (2)). *A configuration  $\boldsymbol{\theta} \in \mathbb{R}^n$  is called a *second-order stationary point* (SOSP) of (2) if  $\nabla E(\boldsymbol{\theta}) = 0$ , and the Hessian  $\mathbf{H}$  is positive semidefinite.*

### 3.3. Correspondence Between the Two Sets of Concepts.

**Proposition 3.6.** *A configuration  $\boldsymbol{\theta} \in \mathbb{R}^n$  is an equilibrium of the Kuramoto model (1) if and only if it is a first-order stationary point of the Kuramoto energy (2).*

*Proof.* This is clear, since both are characterized by

$$\sum_{j=1}^n \mathbf{A}_{ij} \sin(\theta_j - \theta_i) = 0, \quad \forall i \in [n].$$

□

Moreover, since (2) is real analytic, an equilibrium of (1) is stable if and only if it is a local minimum of (2), modulo the global rotation symmetry. Such an equivalence was established in the celebrated work [AK06].

**Definition 3.7** (Local minimum of the energy function). *A configuration  $\boldsymbol{\theta} \in \mathbb{R}^n$  is called a *local minimum* of the energy function  $E(\boldsymbol{\theta})$  if there exists  $\varepsilon > 0$  such that*

$$E(\boldsymbol{\theta}) \leq E(\boldsymbol{\theta}'), \quad \forall \boldsymbol{\theta}' \in \mathbb{R}^n \text{ with } \|\boldsymbol{\theta}' - \boldsymbol{\theta}\| < \varepsilon.$$

Therefore, the relations between stable equilibria, second-order stationary points and local minima can be summarized in Figure 4.

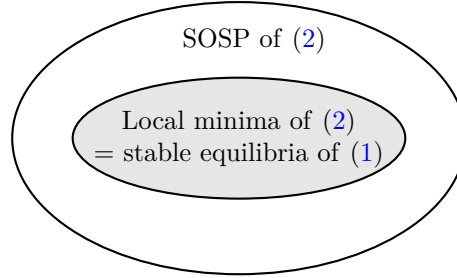


FIGURE 4. Relation between different concepts.

#### 4. VECTOR GEOMETRY OF EQUILIBRIA

In this section, we recast the algebraic conditions introduced in Section 3 into geometric ones, namely combinatorial relations among vectors associated with the nodes. By doing so, the analysis of global synchronization on threshold graphs reduces to reasoning purely about geometric relations between the unit vectors corresponding to the angles in  $\theta$ .

**4.1. Vector-labeled Graph.** Given a state  $\theta \in \mathbb{R}^n$  of the Kuramoto model on graph  $G = (V, E)$ . Associate each node  $i \in V$  its corresponding unit vector

$$\mathbf{v}_i := (\cos \theta_i, \sin \theta_i) \in \mathbb{R}^2.$$

This is called a *phasor*, following the terminology of Yoshiki Kuramoto. The object  $(G, \{\mathbf{v}_i\}_{i \in V})$ , called *vector-labeled graph* encoding  $\theta$  combinatorially and geometrically.

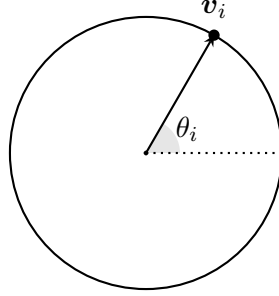


FIGURE 5. Representation of  $\mathbf{v}_i$  with angle  $\theta_i$ .

**4.2. Alignment and Equilibrium.** Given a vector-labeled graph  $(G, \{\mathbf{v}_i\}_{i \in V})$  associated with the state  $\theta$ , we reformulate the equilibrium condition (3) (equivalently (4)) in geometric terms.

**Lemma 4.1** (Equilibrium condition rephrased geometrically). *A state  $\theta$  is an equilibrium of the Kuramoto model (1) on  $G = (V, E)$  with adjacency  $\mathbf{A}$  if and only if, for each  $i \in V$ ,*

$$\sum_{j \in N(i)} \mathbf{v}_j = \mu_i \mathbf{v}_i \quad \text{where} \quad \mu_i = \sum_{j \in N(i)} \cos(\theta_j - \theta_i). \quad (5)$$

where  $\mathbf{v}_i := (\cos \theta_i, \sin \theta_i)$ .

The proof can be found in [MP05], we present here for completeness.

*Proof of Lemma 4.1.* The condition (5) is equivalently written as

$$\sum_{j \in N(i)} e^{i\theta_j} = \mu_i e^{i\theta_i}. \quad (6)$$

Indeed, rewrite all vectors  $\mathbf{v}_i$  in (5) in terms of their Cartesian components, yielding

$$\sum_{j \in N(i)} (\cos \theta_j, \sin \theta_j) = \mu_i (\cos \theta_i, \sin \theta_i).$$

Equivalently,

$$\begin{cases} \sum_{j \in N(i)} \cos \theta_j = \mu_i \cos \theta_i, \\ \sum_{j \in N(i)} \sin \theta_j = \mu_i \sin \theta_i. \end{cases} \quad (7)$$

The condition (7) is equivalent to the equality between the following two complex numbers:

$$\sum_{j \in N(i)} \cos \theta_j + I \sum_{j \in N(i)} \sin \theta_j = \mu_i \cos \theta_i + I \mu_i \sin \theta_i,$$

which can be compactly rewritten as (6) using the Euler formula  $e^{I\theta_i} = \cos \theta_i + I \sin \theta_i$ .

Now that we have derived the equivalence between conditions (5) and (6), our goal reduces to proving the equivalence between (6) and (3), namely

$$\forall i \in V, \quad \sum_{j \in N(i)} e^{I\theta_j} = \mu_i e^{I\theta_i} \iff \sum_{j \in N(i)} \sin(\theta_j - \theta_i) = 0.$$

The implication from the left-hand side to the right-hand side is established by showing that

$$I \sum_{j \in N(i)} \sin(\theta_j - \theta_i) + \sum_{j \in N(i)} \cos(\theta_j - \theta_i) \in \mathbb{R}.$$

This can be verified by a direct computation:

$$\begin{aligned} & I \sum_{j \in N(i)} \sin(\theta_j - \theta_i) + \sum_{j \in N(i)} \cos(\theta_j - \theta_i) \\ &= \sum_{j \in N(i)} e^{I(\theta_j - \theta_i)} \\ &= \frac{\sum_{j \in N(i)} e^{I\theta_j}}{e^{I\theta_i}} \\ &= \mu_i. \end{aligned}$$

To prove the other direction, we construct for every node  $i \in V$ , such a  $\mu_i$  that satisfies the left-hand side. Dividing both sides of (6) by  $e^{I\theta_i}$  (noting that  $e^{I\theta_i} \neq 0$ ), we obtain

$$\frac{\sum_{j \in N(i)} e^{I\theta_j}}{e^{I\theta_i}} = \mu_i.$$

Compute

$$\begin{aligned} \frac{\sum_{j \in N(i)} e^{I\theta_j}}{e^{I\theta_i}} &= \sum_{j \in N(i)} e^{I(\theta_j - \theta_i)} \\ &= \sum_{j \in N(i)} (\cos(\theta_j - \theta_i) + I \sin(\theta_j - \theta_i)) \\ &= \sum_{j \in N(i)} \cos(\theta_j - \theta_i) \end{aligned}$$

where the last equality is due to the fact  $\sum_{j \in N(i)} \sin(\theta_j - \theta_i) = 0$ . Thus

$$\sum_{j \in N(i)} e^{I\theta_j} = \mu_i e^{I\theta_i}$$

holds for every  $i \in V$  by letting  $\mu_i = \sum_{j \in N(i)} \cos(\theta_j - \theta_i)$ .  $\square$

**Remark 4.2** (Normalization and local coherence). *One can rewrite (4.1) into*

$$\mathbf{v}_i = \frac{1}{\mu_i} \sum_{j \in N(i)} \mathbf{v}_j, \quad \text{where } \mu_i = \left\| \sum_{j \in N(i)} \mathbf{v}_j \right\| = \sum_{j \in N(i)} \cos(\theta_j - \theta_i).$$

*The expression describes a geometric condition of equilibrium: At equilibrium, each phasor aligns with the direction of the sum of its neighbors' vectors and is scaled to unit length. Although introduced as a normalization factor, the quantity  $\mu_i$  carries physical meanings. If the neighbors are highly coherent, the sum vector is large, requiring a larger  $\mu_i$  to normalize  $\mathbf{v}_i$  to unit length; if the directions are dispersed,  $\mu_i$  is small. In this sense,  $\mu_i$  measures how strongly the phasors of node  $i$ 's neighbors align directionally. Indeed, defining the local order parameter  $R_i := \frac{1}{\deg(i)} \left| \sum_{j \in N(i)} e^{i\theta_j} \right|$ , we have the relation  $\mu_i = \deg(i) \cdot R_i$ , showing that  $\mu_i$  is proportional to the standard notion of local phase coherence.*

**Remark 4.3** (Equilibrium and force). *This equation admits a natural physical interpretation using the concept of force. Write each phasor  $\mathbf{v}_i$  in complex form as  $e^{i\theta_i}$ . Then, intuitively, each neighboring node  $j \in N(i)$  pulls node  $i$  with a force given by  $e^{I(\theta_j - \theta_i)}$ . Under this interpretation, equation (4.1) states that: At equilibrium, the total force acting on node  $i$  sums to a real scalar. In other words, the net force is purely radial and contributes only to scaling. Due to the unit circle geometry  $|\mathbf{v}_i| = 1$  of the Kuramoto model, such a scaling force does not induce any motion while a tangential component can cause rotation.*

**4.3. Angles and Second-Order Stationarity.** Given an equilibrium  $\boldsymbol{\theta} \in \mathbb{R}^n$  of the Kuramoto model on graph  $G = (V, E)$ , if there exists a node  $i \in V$  whose corresponding  $\mu_i < 0$ , then  $\boldsymbol{\theta}$  cannot be a second-order stationary point of the Kuramoto energy (2). This is because a small perturbation that moves  $\mathbf{v}_i$  toward the direction of  $\sum_{j \in N(i)} \mathbf{v}_j$  strictly decreases the energy.

**Lemma 4.4.** *If  $\boldsymbol{\theta} \in \mathbb{R}^n$  is a second-order stationary point of (2), then for every  $i \in V$  there exists  $\mu_i \geq 0$  such that*

$$\sum_{j \in N(i)} \mathbf{v}_j = \mu_i \mathbf{v}_i.$$

*In particular, either  $\sum_{j \in N(i)} \mathbf{v}_j = \mathbf{0}$  (i.e.,  $\mu_i = 0$ ), or  $\angle\left(\sum_{j \in N(i)} \mathbf{v}_j, \mathbf{v}_i\right) = 0$ .*

*Proof of Lemma 4.4.* By Proposition 3.4, the diagonal entry of the Hessian satisfies

$$\mathbf{H}_{ii} = \sum_{j \in N(i)} \cos(\theta_i - \theta_j).$$

Since  $\theta$  is an equilibrium, we have

$$\sum_{j \in N(i)} \sin(\theta_j - \theta_i) = 0,$$

which implies that

$$\sum_{j \in N(i)} e^{i(\theta_j - \theta_i)} = \sum_{j \in N(i)} \cos(\theta_j - \theta_i) \in \mathbb{R}.$$

By Lemma 4.1, this real quantity equals  $\mu_i$  at first-order stationary point  $\boldsymbol{\theta}$ . Hence  $\mathbf{H}_{ii} = \mu_i$ . If  $\mu_i < 0$ , then  $\mathbf{H}_{ii} < 0$ , contradicting the positive semidefiniteness of  $\mathbf{H}$ .  $\square$

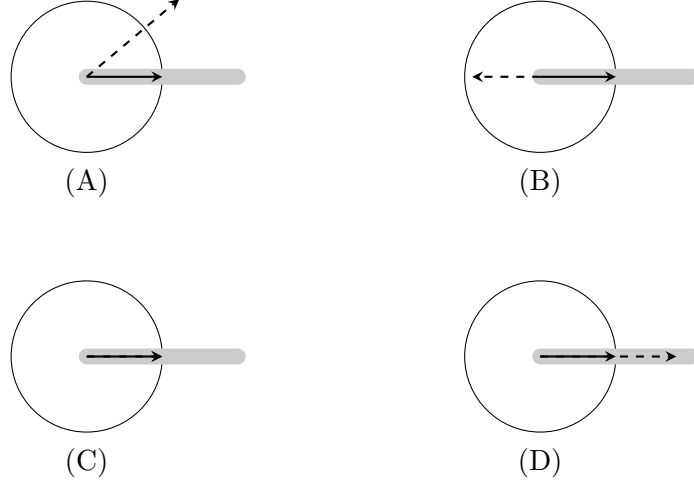


FIGURE 6. The solid arrow represents  $\mathbf{v}_i$ , and the dashed arrow represents  $\sum_{j \in N(i)} \mathbf{v}_j$ . For each node  $i$ , the four panels show all possible relations between  $\mathbf{v}_i$  and  $\sum_{j \in N(i)} \mathbf{v}_j$ . Among them, case (A) violates the first-order condition, while case (B) violates the second-order stationary condition, since the aggregated phasor  $\sum_{j \in N(i)} \mathbf{v}_j$  lies outside the feasible (gray) region corresponding to  $\mu_i \geq 0$ .

The geometric conditions of second-order stationary points presented here are only the most basic one. Further necessary geometric conditions will be established in subsequent sections, and these will be essential for showing that every connected threshold graph is globally synchronizing.

## 5. LOCAL SYNCHRONIZATION PRIMITIVES

**5.1. A Fundamental Geometric Fact.** We begin with a geometric lemma that characterizes all possible relative positions of two unit vectors satisfying a pair of linear relations. This fact will serve as the local synchronization primitive used in the induction argument in Section 6.

**Lemma 5.1.** *Let  $\mathbf{v}_a, \mathbf{v}_b \in \mathbb{S}^1$ . Suppose there exist a vector  $\mathbf{q} \in \mathbb{R}^2$  and scalars  $\mu_a, \mu_b \in \mathbb{R}$  such that*

$$\mathbf{v}_b + \mathbf{q} = \mu_a \mathbf{v}_a \quad \text{and} \quad \mathbf{v}_a + \mathbf{q} = \mu_b \mathbf{v}_b. \quad (8)$$

*Then the positions of  $\mathbf{v}_a$  and  $\mathbf{v}_b$  fall into one of the following three cases:*

- (1)  $\mathbf{v}_a = \mathbf{v}_b$  and  $\mu_a = \mu_b$ ;
- (2)  $\mathbf{v}_a = -\mathbf{v}_b$ ,  $\mu_a + \mu_b = -2$ , and  $(\mu_a, \mu_b) \neq (-1, -1)$ ;
- (3)  $\mathbf{v}_a, \mathbf{v}_b \in \mathbb{S}^1$ ,  $\mu_a = \mu_b = -1$ , and  $\mathbf{v}_a + \mathbf{v}_b + \mathbf{q} = 0$ .

*Proof.* According to (8), we have

$$\mathbf{q} = \mu_a \mathbf{v}_a - \mathbf{v}_b = \mu_b \mathbf{v}_b - \mathbf{v}_a$$

Thus

$$(\mu_a + 1)\mathbf{v}_a = (\mu_b + 1)\mathbf{v}_b. \quad (9)$$

*Case 1:*  $\mu_a \neq -1$  and  $\mu_b \neq -1$ . In this case, from (9), it must hold that

$$\mathbf{v}_a \parallel \mathbf{v}_b.$$

This leads to two subcases:

- (1.1) If  $\mu_a = \mu_b \neq -1$ , then  $\mathbf{v}_a = \mathbf{v}_b$ ;
- (1.2) If  $\mu_a + 1 = -(\mu_b + 1)$ , then equivalently, we have  $\mu_a + \mu_b = -2$ . This implies  $\mathbf{v}_a = -\mathbf{v}_b$ .

Case 2:  $\mu_a = \mu_b = -1$ . In this case, we have

$$\mathbf{q} + \mathbf{v}_a + \mathbf{v}_b = \mathbf{0}.$$

□

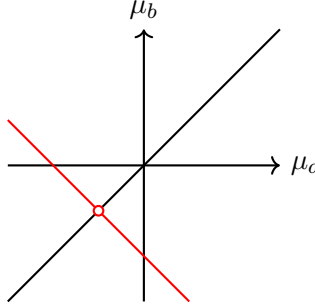


FIGURE 7. The feasible region for  $(\mu_a, \mu_b)$  consists of: (1) the black line  $\mu_a = \mu_b$ , excluding the intersection point, corresponding to  $\mathbf{v}_a = \mathbf{v}_b$ ; (2) the red line  $\mu_a + \mu_b = -2$ , excluding the intersection point, corresponding to the antipodal case  $\mathbf{v}_a = -\mathbf{v}_b$ ; (3) their intersection point  $(-1, -1)$ , marked by a hollow dot, at which no additional constraint is imposed on the vectors  $\mathbf{v}_a$  and  $\mathbf{v}_b$ .

**Corollary 5.2.** *Under the assumptions of Lemma 5.1, if in addition  $\mu_a, \mu_b \geq 0$ , then  $\mathbf{v}_a = \mathbf{v}_b$ .*

*Proof.* With  $\mu_a, \mu_b \geq 0$ , Lemma 5.1 leaves only case (1.1), hence  $\mathbf{v}_a = \mathbf{v}_b$ . □

We introduce a geometric analogue of the notion of twins in graph theory, tailored to the Kuramoto model.

**Definition 5.3** (Geometrically closed twins). Motivated by the notion of closed twins in graph theory, we say that, at a state  $\boldsymbol{\theta}$  of the Kuramoto model on  $G$ , nodes  $i$  and  $j$  are called *geometrically closed twins* if their phasors  $\mathbf{v}_i$  and  $\mathbf{v}_j$  satisfy the relations of Lemma 5.1.

**Definition 5.4** (Geometrically stable closed twins). We say that, at a state  $\boldsymbol{\theta}$  of the Kuramoto model on  $G$ , nodes  $i$  and  $j$  are called *geometrically stable closed twins* if their phasors  $\mathbf{v}_i$  and  $\mathbf{v}_j$  satisfy the relations of Lemma 5.1 and, in addition,  $\mu_i, \mu_j \geq 0$ .

## 5.2. Phasor Geometry of Closed Twins.

**Definition 5.5.** Let  $G = (V, E)$  be a graph. Two nodes  $i, j \in V$  are called *closed twins* if

$$N[i] = N[j], \tag{10}$$

where  $N[i]$  is defined as  $N(i) \cup \{i\}$ .

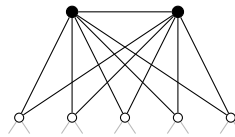


FIGURE 8. The two black nodes form a pair of closed twins.

Open twins, corresponding to  $N(i) = N(j)$ , will not be needed in this work.

**Corollary 5.6.** Let  $\boldsymbol{\theta} \in \mathbb{R}^n$  be a second-order stationary point of the energy function  $E_G(\boldsymbol{\theta})$ . If nodes  $a$  and  $b$  form a pair of closed twins (satisfying (10)), then  $\mathbf{v}_a = \mathbf{v}_b$ .

*Proof.* From Lemma 4.4, since  $\boldsymbol{\theta}$  is a second-order stationary point, there exist  $\mu_a, \mu_b \geq 0$  such that

$$\begin{cases} \sum_{j \in N(a)} \mathbf{v}_j = \mu_a \mathbf{v}_a, \\ \sum_{j \in N(b)} \mathbf{v}_j = \mu_b \mathbf{v}_b. \end{cases}$$

Because  $N[a] = N[b]$ , we have  $N(a) \setminus \{b\} = N(b) \setminus \{a\}$ , and we denote this common set by  $M$ . Thus,

$$\begin{cases} \sum_{j \in M} \mathbf{v}_j + \mathbf{v}_b = \mu_a \mathbf{v}_a, \\ \sum_{j \in M} \mathbf{v}_j + \mathbf{v}_a = \mu_b \mathbf{v}_b. \end{cases}$$

By Corollary 5.2 and the fact that  $\mu_a, \mu_b \geq 0$ , we conclude that  $\mathbf{v}_a = \mathbf{v}_b$ .  $\square$

Clearly, this is a case where geometric twins defined in (5.4) formed.

Moreover, Corollary 5.6 implies immediately that windmill graphs are globally synchronizing.

**Theorem 5.7.** Every windmill graph is globally synchronizing.

*Proof.* Let  $G$  be a windmill graph  $W_{p,m}$  with central vertex  $c$ . Then there exists a partition of the vertex set

$$V \setminus \{c\} = \biguplus_{\ell=1}^m S_\ell$$

such that each induced subgraph  $G[S_\ell]$  is a clique, and every vertex in  $S_\ell$  is adjacent to  $c$ . For each  $\ell$ , all vertices in  $S_\ell$  have identical closed neighborhoods and therefore form a class of closed twins. By Corollary 5.6, all vertices in each  $S_\ell$  must share the same phase. According to Lemma (4.4), we have for  $\forall i \in S_\ell$ , that

$$\mathbf{v}_i \uparrow \mathbf{v}_c + \sum_{j \in S_\ell, j \neq i} \mathbf{v}_j \quad \text{or} \quad \mathbf{v}_c + \sum_{j \in S_\ell, j \neq i} \mathbf{v}_j = \mathbf{0}.$$

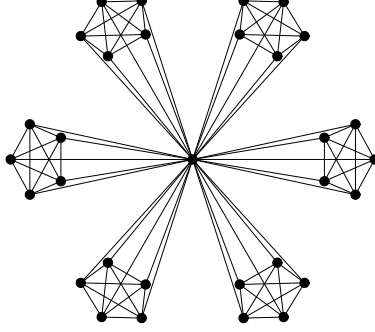
We distinguish two cases.

*Case 1.*  $\mathbf{v}_c \uparrow \mathbf{v}_i + \sum_{j \in S_\ell, j \neq i} \mathbf{v}_j$ . It is then clear that either  $\mathbf{v}_c = \mathbf{v}_i$  or  $\mathbf{v}_c = -\mathbf{v}_i$  holds. If  $\mathbf{v}_c = -\mathbf{v}_i$ , then  $\boldsymbol{\theta}$  is not a second-order stationary point. Indeed, let  $\mathbf{x} \in \mathbb{R}^n$  be the vector whose  $i$ -th component equals 1 if  $i \in S_\ell$  and 0 otherwise. Then

$$\begin{aligned} \mathbf{x}^\top \mathbf{H} \mathbf{x} &= \frac{1}{2} \sum_{i=1}^n \sum_{j=1}^n \mathbf{A}_{ij} \cos(\theta_i - \theta_j) (x_i - x_j)^2 \\ &= \sum_{i \in S_\ell} \sum_{j \in V \setminus S_\ell} \mathbf{A}_{ij} \cos(\theta_i - \theta_j) \\ &= \sum_{i \in S_\ell} \cos(\theta_i - \theta_c) < 0, \end{aligned}$$

which contradicts the positive semidefiniteness of  $\mathbf{H}$ .

*Case 2.*  $\mathbf{v}_c + \sum_{j \in S_\ell, j \neq i} \mathbf{v}_j = \mathbf{0}$ . Then necessarily  $|S_\ell| = 2$ . In this case, the phasors of the two nodes in  $S_\ell$  are opposite to  $\mathbf{v}_c$ . By an argument analogous to the one above, the matrix  $\mathbf{H}$  is not positive semidefinite.  $\square$

FIGURE 9. Windmill graphs  $W_{5,6}$ .

**5.3. Synchronous Pendant Extension.** In this section, we present Lemma 5.9 which describes a scenario where a group of nodes forms geometrically stable closed twins 5.4 without being closed twins in the graph-theoretic sense. Before that, we establish Lemma 5.8, which serves as a preparatory step.

**Lemma 5.8.** *Let  $G = (V, E)$  be a graph, and let  $W \subseteq V$  admit a partition*

$$W = Q \uplus S \uplus P,$$

*with the following structural conditions:*

- (1) *Every node in  $Q$  has all its neighbors inside  $S$ , i.e.,  $N(i) \subseteq S$  for all  $i \in Q$ ;*
- (2) *The vertex set  $S \subseteq V(G)$  induces a clique in  $G$ ;*
- (3) *For each  $i \in S$ , its neighborhood is  $P \uplus N_Q(i) \uplus (S \setminus \{i\})$ , where*

$$N_Q(i) = \{q \in Q : q \sim i\}.$$

*Assume further that  $\{\mathbf{v}_i\}_{i \in V}$  is the vector configuration corresponding to any second-order stationary point  $\boldsymbol{\theta}$  of the Kuramoto energy (2), and that the induced subgraph on  $Q \uplus S$  is synchronized at  $\boldsymbol{\theta}$ , namely  $\mathbf{v}_i = \mathbf{v}$  for all  $i \in Q \uplus S$ , for some common phasor  $\mathbf{v}$ . Then the phasor sum over  $P$  satisfies*

$$\sum_{i \in P} \mathbf{v}_i \uparrow \mathbf{v} \quad \text{or} \quad \sum_{i \in P} \mathbf{v}_i = \mathbf{0}.$$

*Proof.* For any node  $i \in S$ ,

$$N(i) = N_Q(i) \uplus (S \setminus \{i\}) \uplus P \tag{11}$$

and

$$\sum_{j \in N(i)} \mathbf{v}_j = \mu_i \mathbf{v}_i, \quad \mu_i \geq 0. \tag{12}$$

Plug (11) into (12), we obtain

$$\sum_{j \in N_Q(i) \uplus (S \setminus \{i\}) \uplus P} \mathbf{v}_j = \mu_i \mathbf{v}_i, \quad \mu_i \geq 0$$

Since  $Q \uplus S$  forms a synchronized group, we have

$$(|N_Q(i)| + |S| - 1) \mathbf{v}_i + \sum_{j \in P} \mathbf{v}_j = \mu_i \mathbf{v}_i, \quad \mu_i \geq 0. \tag{13}$$

Thus

$$\sum_{j \in P} \mathbf{v}_j = (\mu_i - (|N_Q(i)| + |S| - 1)) \mathbf{v}_i, \quad \mu_i \geq 0.$$

In fact,  $\mu_i - (|N_Q(i)| + |S| - 1) < 0$  does not hold, because in this case there exists a direction along which the energy decreases in a neighborhood of  $\boldsymbol{\theta}$ . To see this, let  $\mathbf{x}$  be the  $n$ -dimensional indicator

vector of  $Q \uplus S$ , i.e.,  $\mathbf{x}_i = 1$  for  $i \in Q \uplus S$  and  $\mathbf{x}_i = 0$  otherwise. Since  $\mu_i - (|N_Q(i)| + |S| - 1) < 0$ , we have  $\langle \sum_{j \in P} \mathbf{v}_j, \mathbf{v}_i \rangle < 0$ . Thus

$$\begin{aligned}
\mathbf{x}^T H \mathbf{x} &= \frac{1}{2} \sum_{i=1}^n \sum_{j=1}^n \mathbf{A}_{ij} \cos(\theta_i - \theta_j) (x_i - x_j)^2 \\
&= \sum_{i \in Q \uplus S} \sum_{j \in V \setminus (Q \uplus S)} \mathbf{A}_{ij} \cos(\theta_i - \theta_j) (x_i - x_j)^2 \\
&= \sum_{i \in S} \sum_{j \in P} \cos(\theta_i - \theta_j) (x_i - x_j)^2 \\
&= \sum_{i \in S} \sum_{j \in P} \cos(\theta_i - \theta_j) \\
&= \sum_{i \in S} \sum_{j \in P} \mathbf{v}_i \cdot \mathbf{v}_j \\
&= \sum_{i \in S} \mathbf{v}_i \cdot \sum_{j \in P} \mathbf{v}_j \\
&= |S| \mathbf{v}_i \cdot \sum_{j \in P} \mathbf{v}_j.
\end{aligned} \tag{14}$$

Clearly, if  $\mu_i - (|N_Q(i)| + |S| - 1) < 0$ , then (13) implies that

$$\mathbf{v}_i \cdot \sum_{j \in P} \mathbf{v}_j < 0.$$

Consequently, the quantity (14) is negative, which contradicts the second-order stationarity of the state  $\theta$ .  $\square$

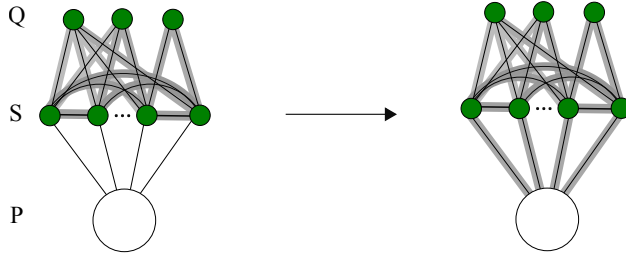


FIGURE 10. Illustration of Lemma 5.8. The green vertices correspond to nodes for which  $\mu_i \mathbf{v}_i = \sum_{j \in N(i)} \mathbf{v}_j$  holds with  $\mu_i \geq 0$ . The large circular node represents the set  $P$  of vertices. Gray-shaded edges between two nodes indicate that the vectors corresponding to these two nodes are synchronized. The structural relations among the sets  $Q$ ,  $S$ , and  $P$ , together with the synchronization of  $Q \uplus S$ , imply a synchronization in phase between  $Q \uplus S$  and the phasor sum over  $P$ .

**Lemma 5.9.** *Let  $G = (V, E)$  be a graph, and let  $W \subseteq V$  admit a partition*

$$W = Q \uplus S_1 \uplus S_2 \uplus P$$

*with the following structural conditions:*

- (i) *Every node in  $Q$  has all its neighbors inside  $S_1$ , i.e.,  $N(i) \subseteq S_1$  for all  $i \in Q$ ;*
- (ii) *The vertex set  $S_1 \uplus S_2 \subseteq V(G)$  induces a clique in  $G$ ;*
- For each  $i \in S_1 \uplus S_2$ , its neighborhood is  $P \uplus N_Q(i) \uplus (S \setminus \{i\})$ , where*

$$N_Q(i) = \{q \in Q : q \sim i\}.$$

(iii) For any  $i \in S_1 \uplus S_2$ , its neighbourhood can be decomposed into three parts: the set  $P$ , its neighbours inside  $Q$ , and the rest of the clique  $S_1 \uplus S_2$ . That is

$$N(i) = P \uplus N_Q(i) \uplus ((S_1 \uplus S_2) \setminus \{i\}).$$

Assume further that  $\{\mathbf{v}_i\}_{i \in V}$  corresponds to a second-order stationary point  $\boldsymbol{\theta}$  of the Kuramoto energy (2), at which the induced subgraph on  $Q \uplus S_1$  is synchronized, i.e.,

$$\mathbf{v}_i = \mathbf{v}, \quad \forall i \in Q \uplus S_1,$$

for some common phasor  $\mathbf{v}$ . Then the set  $S_1 \uplus S_2$  synchronize.

*Proof.* *Step A.* Observe that the set  $S_1$  induces a clique, and  $Q \uplus S_1$  forms a synchronizing group. Hence by Lemma 5.8, for every  $i \in S_1$  there exists  $\mu_i \geq 0$  such that

$$\sum_{k \in S_2 \uplus P} \mathbf{v}_k = \mu_i \mathbf{v}_i. \quad (15)$$

*Step B.* Since  $S_1$  is a synchronizing group, we have

$$\sum_{k \in S_1 \setminus \{i\}} \mathbf{v}_k = (|S_1| - 1) \mathbf{v}_i.$$

Adding this term to (15) yields

$$\sum_{k \in S_2 \uplus P \uplus (S_1 \setminus \{i\})} \mathbf{v}_k = (\mu_i + |S_1| - 1) \mathbf{v}_i.$$

where  $\mu_i + |S_1| - 1 > 0$ . In other words,

$$\forall i \in S_1, \quad \mathbf{v}_i \uparrow \sum_{k \in S_2 \uplus P \uplus (S_1 \setminus \{i\})} \mathbf{v}_k. \quad (16)$$

*Step C.* According to Lemma 4.4, nodes in the set  $S_2$  satisfy

$$\forall i \in S_2, \quad \mathbf{v}_i \uparrow \sum_{k \in S_1 \uplus P \uplus S_2 \setminus \{i\}} \mathbf{v}_k \quad \text{or} \quad \sum_{k \in S_1 \uplus P \uplus S_2 \setminus \{i\}} \mathbf{v}_k = \mathbf{0}. \quad (17)$$

since  $\boldsymbol{\theta}$  is a second-order stationary point. Combining (16) and (17), we deduce that all nodes in  $S_1 \uplus S_2$  are geometrically stable twins in the sense of Definition 5.4. It then follows from Corollary 5.2 that  $S_1 \uplus S_2$  forms a synchronizing group.  $\square$

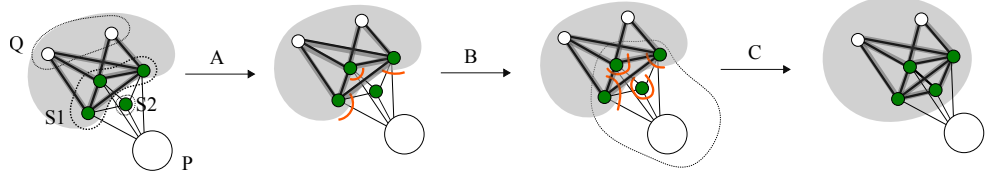


FIGURE 11. Illustration of the proof of Lemma 5.9, illustrating how the synchronized block  $Q \uplus S_1$  extends to include  $S_2$  through propagation enabled by the specific local structure. The green vertices correspond to nodes for which  $\mu_i \mathbf{v}_i = \sum_{j \in N(i)} \mathbf{v}_j$  holds with  $\mu_i \geq 0$ . The gray-shaded nodes are synchronized; an edge with a gray background indicates synchronization between the corresponding nodes. Each orange arc separates a small green node from a group of nodes it connects to, indicating that the vector of the green node is in the same direction as the sum of the vectors of the nodes on the opposite side of the arc.

## 6. MAIN PROOF: THE INDUCTION ARGUMENT

**6.1. A Prototype Example.** Let us take a look at the threshold graph corresponding to the sequence 01010101. The first vertex is denoted by  $A$ , and we label the vertices  $A$  through  $I$  in the order in which they appear in the sequence.

Let  $G$  be the threshold graph corresponding to the sequence 01010101. To prove that  $G$  is globally synchronizing, we show that every second-order stationary point  $\theta$  of  $E_G(\theta)$  is synchronous; that is,  $\theta_1 = \dots = \theta_n$ .

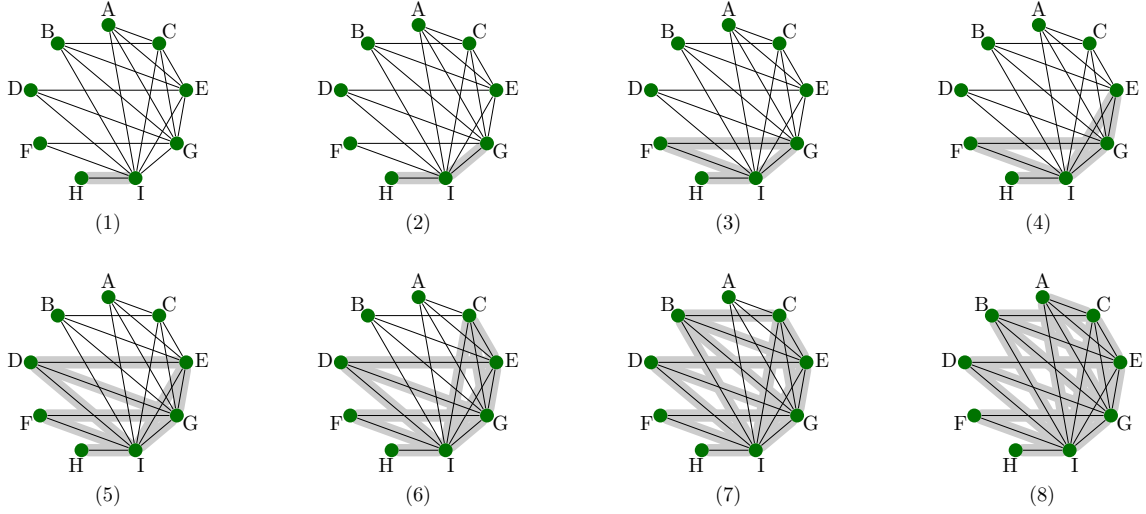


FIGURE 12. Synchronization propagates in eight steps, forcing every second-order stationary point to be synchronous. Gray-shaded edges represent synchronizing relations that have been established at each step.

*Step (1)* We begin with the edge between  $H$  and  $I$ . Applying Lemma 4.4 to node  $H$  shows that, since  $\theta$  is a second-order stationary point, we must have  $\mathbf{v}_H \uparrow \mathbf{v}_I$ . Equivalently,

$$\theta_H = \theta_I.$$

*Step (2)* Observe that  $N(G) = N(I) \cup \{H\}$  and  $\theta_H = \theta_I$ , applying Lemma 5.9 by letting  $Q = \{H\}$ ,  $S_1 = \{I\}$ ,  $S_2 = \{G\}$ ,  $P = \{F, D, B, A, C, E\}$ , we obtain

$$\theta_G = \theta_I.$$

Intuitively, the only difference between the neighborhoods of  $G$  and  $I$  is that  $I$  has one additional neighbor, namely  $H$ . This extra neighbor does not obstruct the synchronization between  $G$  and  $I$ , because  $H$  is already synchronized with  $I$  and therefore behaves as a synchronous pendant at this stage.

*Step (3)* Note that node  $F$  connects only to  $G$  and  $I$ , which are synchronized as established in Step (2). Therefore, by Lemma 4.4, we have

$$\theta_F = \theta_G = \theta_I.$$

*Step (4)* Applying Lemma 5.9 with  $Q = \{F, H\}$ ,  $S_1 = \{G, I\}$ ,  $S_2 = \{E\}$ , and  $P = \{D, B, A, C\}$ , we conclude

$$\theta_E = \theta_G = \theta_I.$$

*Step (5)* Note that node  $D$  connects to  $E$ ,  $G$ , and  $I$ , which are synchronized as established in Step (4). Therefore, by Lemma 4.4, we have

$$\theta_D = \theta_E = \theta_G = \theta_I.$$

*Step (6)* Applying Lemma 5.9 with  $Q = \{D, F, H\}$ ,  $S_1 = \{E, G, I\}$ ,  $S_2 = \{C\}$ , and  $P = \{A, B\}$ , we conclude

$$\theta_C = \theta_E = \theta_G = \theta_I.$$

*Step (7)* Note that node  $B$  connects to  $C, E, G$ , and  $I$ , which are synchronized as established in Step (6). Therefore, by Lemma 4.4, we have

$$\theta_B = \theta_C = \theta_E = \theta_G = \theta_I.$$

*Step (8)* As in Step (7), Lemma 4.4 implies that

$$\theta_A = \theta_C = \theta_E = \theta_G = \theta_I$$

since these nodes form a synchronizing group and constitute all neighbors of  $A$ .

In conclusion, every second-order stationary point  $\theta$  is a fully synchronized state. Hence the threshold graph corresponding to 01010101 is globally synchronizing.

## 6.2. Proof of Theorem 1.2: General Case.

*Proof of Theorem 1.2.* Any connected threshold graph can be described by a bit sequence of 1's and 0's, where the last bit must be a 1; otherwise, the threshold graph is not connected. For simplicity, we decompose the sequence into maximal contiguous blocks of 1's and 0's:

$$U_1, I_2, U_2, \dots, I_{k-1}, U_{k-1}, I_k, U_k,$$

or

$$I_1, U_1, I_2, U_2, \dots, I_{k-1}, U_{k-1}, I_k, U_k,$$

where  $U_i$  denotes a subsequence of 1's and  $I_i$  denotes a subsequence of 0's. Without loss of generality, we focus on threshold graphs  $G = (V, E)$  of the first sequence type; the second case follows by an entirely analogous argument.

Let  $\theta$  be a second-order stationary point of the energy function  $E_G(\theta)$  of the homogeneous Kuramoto model on  $G$ . We prove that  $\theta$  is a fully synchronized state by induction on  $m$ , where  $m$  denotes the number of 1-blocks counted from the end of the threshold sequence.

For the base case, observe that all nodes within a block of 1's form a set of closed twins. Hence, at any second-order stationary point  $\theta$ , the nodes in the last block  $U_k$  must synchronize, as follows directly from Corollary 5.6.

Assume as the inductive hypothesis that the nodes in the last  $m$  blocks of 1's,  $U_{k-m+1}, \dots, U_k$ , are synchronized, i.e., there exists a common phasor  $\mathbf{v}$  such that  $\mathbf{v}_i = \mathbf{v}$  for all  $i \in U_{k-m+1} \uplus \dots \uplus U_k$ . Lemma 4.4 then implies that the nodes in the adjacent 0-blocks  $I_{k-m+1} \uplus \dots \uplus I_k$  also satisfy  $\mathbf{v}_i = \mathbf{v}$ .

Define

$$\begin{aligned} Q &:= I_{k-m+1} \uplus \dots \uplus I_k, \\ S_1 &:= U_{k-m+1} \uplus \dots \uplus U_k, \\ S_2 &:= U_{k-m}, \\ P &:= U_1 \uplus \dots \uplus U_{k-m-1} \uplus I_2 \uplus \dots \uplus I_{k-m}. \end{aligned}$$

We now verify that the assumptions of Lemma 5.9 are satisfied by the above decomposition, which follows directly from the threshold construction.

By construction, the vertices in  $Q$  correspond to the most recent 0-blocks preceding  $S_1$ . Hence, every vertex in  $Q$  is adjacent only to vertices in  $S_1$ . Moreover, since  $S_1$  and  $S_2$  consist of consecutive dominating blocks, the induced subgraph on  $S_1 \cup S_2$  is a clique. Finally, for each  $i \in S_1$ , its neighborhood can be decomposed as

$$N(i) = P \uplus ((S_1 \cup S_2) \setminus \{i\}) \uplus N_Q(i),$$

where  $P$  denotes the set of vertices added earlier in the construction. Hence, all the assumptions of Lemma 5.9 are satisfied, and we conclude that the sets  $S_1$  and  $S_2$  synchronize. In other words, the last  $m + 1$  blocks of 1's  $U_{k-m}, U_{k-m+1}, \dots, U_k$  synchronize.

Therefore, every second-order stationary point is a synchronous state, and it follows that  $G$  is globally synchronizing.  $\square$

## 7. DISCUSSION: BEYOND DENSITY-BASED GUARANTEES

As noted in the introduction, previous guarantees for global synchronization have largely focused on minimum-degree conditions: that is, requiring every node to be connected to more than a fixed fraction of the remaining vertices. In this regime, graphs are necessarily highly dense, and their degree sequences are relatively homogeneous. This naturally raises the question:

*Does a graph that exhibits global synchronization necessarily have high edge density or a nearly regular degree sequence (i.e., with small degree variability)?*

In this section, we provide a negative answer to this question<sup>4</sup> by showing that threshold graphs realize every admissible edge density, and that their degree sequences are extremal in the sense that they majorize any other degree sequence.

**7.1. Threshold Graphs Realize All Densities.** The edge density of a graph  $G$  on  $n$  vertices takes values in

$$\text{density}(G) \in \left\{ \frac{m}{\binom{n}{2}} \mid m \in \{0, \dots, \binom{n}{2}\} \right\}. \quad (18)$$

Moreover, for connected graphs, the edge density takes values corresponding to

$$m \in \{n-1, \dots, \binom{n}{2}\}.$$

The following lemma shows that every admissible edge density can be realized by a threshold graph.

**Lemma 7.1.** *For any pair of integers  $n > 0$  and  $0 \leq m \leq \binom{n}{2}$ , there is a threshold graph with  $n$  vertices and  $m$  edges. If  $m \geq n-1$ , there is a connected threshold graph with  $n$  vertices and  $m$  edges.*

*Proof.* The proof is by induction over  $n$ . For the base case, note that the only graph with  $n = 1$  vertex has  $0 = m = \binom{n}{2}$  edges and is connected by definition. For  $n > 1$ , we consider two cases:

- If  $m < n-1$ , the induction hypothesis implies that there is a threshold graph with  $n-1 \geq 1$  vertices and  $m < n-1 \leq \binom{n-1}{2}$  edges to which an isolated vertex can be added to obtain a threshold graph with  $n$  vertices and  $m$  edges.
- Otherwise, the induction hypothesis implies that there is a threshold graph with  $m - (n-1) \leq \binom{n-1}{2}$  edges to which a universal vertex can be added to obtain a connected threshold graph with  $n$  vertices and  $m$  edges.

$\square$

**7.2. Degree Sequence of Threshold Graphs.** One way to compare how spread out the degree sequences of two graphs are is through majorization. Let  $G$  and  $G'$  be two graphs with the same edge density, and let

$$\mathbf{d}(G) = (d_1, \dots, d_n), \quad \mathbf{d}(G') = (d'_1, \dots, d'_n)$$

denote their degree sequences arranged in nonincreasing order. We say that  $\mathbf{d}(G)$  *majorizes*  $\mathbf{d}(G')$ , and write  $\mathbf{d}(G) \succ \mathbf{d}(G')$ , if

$$\sum_{i=1}^k d_i \geq \sum_{i=1}^k d'_i \quad \text{for all } k = 1, \dots, n-1,$$

---

<sup>4</sup>Of course, trees provide trivial examples.

and

$$\sum_{i=1}^n d_i = \sum_{i=1}^n d'_i.$$

The following is a classical result on degree sequence (called a *threshold sequence*) of threshold graphs.

**Theorem 7.2** ([PS89]). *A degree sequence  $\mathbf{d}$  is a threshold sequence if and only if it is not strictly majorized by any other graphical degree sequence.*

This theorem formalizes the intuition that threshold graphs are extremal, in the sense that their degree mass is concentrated as much as possible on high-degree vertices.

## 8. SUMMARY AND OPEN PROBLEMS

In this work, we identify threshold graphs as a class of interaction networks that are globally synchronizing, despite spanning the full range of admissible edge densities from  $2/n$  to 1. This significantly extends existing sufficient conditions for global synchronization, which are largely restricted to graphs with high minimum degree or uniformly dense connectivity.

Our analysis crucially exploits the constructive nature of threshold graphs: they form the smallest graph class closed under the successive addition of isolated and universal nodes. This closure property enables an inductive approach, whereby global synchronization is shown to be preserved when starting from a smaller synchronizing threshold graph and adding either an isolated node or a universal node. From a geometric perspective, this reveals a local-to-global propagation mechanism, whereby synchronization constraints imposed on a small subset of nodes progressively force synchrony across the entire network.

A natural question is whether this closure phenomenon extends beyond threshold graphs. Specifically, suppose  $G$  is an arbitrary globally synchronizing graph. If we add a universal node to  $G$ , is the resulting graph still globally synchronizing? We expect the answer to be yes, since attaching a node that is connected to all existing vertices does not appear to introduce new geometric directions for the oscillators beyond the synchronized configuration. However, we do not currently know how to prove this, and we leave this problem for future work.

Moreover, we expect that our results may admit further generalizations. Possible directions include extending the analysis to oscillators evolving on higher-dimensional spheres, incorporating nonlinear interaction terms as in [GLPR25], and considering broader classes of graphs. For instance, one may study systems in which oscillators are coupled through both positive and negative edges.

**Acknowledgements.** We would like to thank Afonso S. Bandeira for insightful discussions and Kevin Lucca for pointing out relevant references on the known bounds of the density threshold.

## REFERENCES

- [ABK<sup>+</sup>26] Pedro Abdalla, Afonso S. Bandeira, Martin Kassabov, Victor Souza, Steven H. Strogatz, and Alex Townsend. Expander graphs are globally synchronizing. *Adv. Math.*, 488:110773, 2026.
- [ABPV<sup>+</sup>05] Juan A Acebrón, L L Bonilla, Conrad J Pérez Vicente, Félix Ritort, and Renato Spigler. The kuramoto model: A simple paradigm for synchronization phenomena. *Rev. Mod. Phys.*, 77(1):137–185, 2005.
- [AK06] P.-A. Absil and K. Kurdyka. On the stable equilibrium points of gradient systems. *Syst. Control. Lett.*, 55(7):573–577, 2006.
- [AMP77] Giorgio Ausiello, Alberto Messina, and Giuseppe Protasi. A graph-theoretic characterization of the pv-chunk class of synchronizing primitives. *SIAM J. Comput.*, 6(1):88–108, 1977.
- [BB68] John Buck and Elisabeth Buck. Mechanism of rhythmic synchronous flashing of fireflies. *Science*, 159(3821):1319–1327, 1968.
- [BBV16] Afonso S Bandeira, Nicolas Boumal, and Vladislav Voroninski. On the low-rank approach for semidefinite programs arising in synchronization and community detection. In *Conference on learning theory*, pages 361–382. PMLR, 2016.

[BKMR25] Afonso S. Bandeira, Anastasia Kireeva, Antoine Maillard, and Almut Rödder. Randomstrasse101: Open problems of 2024. Preprint, 2025.

[Can22] Eduardo A. Canale. From weighted to unweighted graphs in synchronizing graph theory. Preprint, 2022.

[CCC95] H.-D. Chiang, C. C. Chu, and G. Cauley. Direct stability analysis of electric power systems using energy functions: Theory, applications, and perspective. *Proc. IEEE*, 83(11):1497–1529, 1995.

[CH77a] Václav Chvátal and Peter L. Hammer. Aggregations of inequalities. In *Studies in Integer Programming*, volume 1 of *Annals of Discrete Mathematics*, pages 145–162. North-Holland, Amsterdam, 1977.

[CH77b] Václav Chvátal and Peter L. Hammer. *Threshold Graphs and Related Topics*. Annals of Discrete Mathematics. North-Holland, 1977.

[CRMB24] Christopher Criscitiello, Quentin Rebjock, Andrew D. McRae, and Nicolas Boumal. Synchronization on circles and spheres with nonlinear interactions. Preprint, 2024.

[DB12] Florian Dörfler and Francesco Bullo. Synchronization and transient stability in power networks and non-uniform kuramoto oscillators. *SIAM J. Control Optim.*, 50(3):1616–1642, 2012.

[DB14] Florian Dörfler and Francesco Bullo. Synchronization in complex networks of phase oscillators: A survey. *Automatica*, 50(6):1539–1564, 2014.

[GLPR23] Borjan Geshkovski, Cyril Letrouit, Yury Polyanskiy, and Philippe Rigollet. The emergence of clusters in self-attention dynamics. In *Advances in Neural Information Processing Systems*, pages 57026–57037, 2023.

[GLPR25] Borjan Geshkovski, Cyril Letrouit, Yury Polyanskiy, and Philippe Rigollet. A mathematical perspective on transformers. *Bull. Amer. Math. Soc.*, 62(3):427–479, 2025.

[JMS25] Vishesh Jain, Clayton Mizgerd, and Mehtaab Sawhney. The random graph process is globally synchronizing. *Bull. Lond. Math. Soc.*, 2025.

[Kha02] Hassan K. Khalil. *Nonlinear Systems*. Prentice Hall, Upper Saddle River, NJ, 3rd edition, 2002.

[KST21] Martin Kassabov, Steven H. Strogatz, and Alex Townsend. Sufficiently dense kuramoto networks are globally synchronizing. *Chaos*, 31(7):073135, 2021.

[KST22] Martin Kassabov, Steven H Strogatz, and Alex Townsend. A global synchronization theorem for oscillators on a random graph. *Chaos*, 32(9):093119, 2022.

[Kur75] Yoshiki Kuramoto. Self-entrainment of a population of coupled non-linear oscillators. In *International Symposium on Mathematical Problems in Theoretical Physics*, pages 420–422. Springer, 1975.

[Lag07] Christian Lageman. Pointwise convergence of gradient-like systems. *Math. Nachr.*, 280(13–14):1543–1558, 2007.

[Lin25] Shuyang Ling. Local geometry determines global landscape in low-rank factorization for synchronization. *Found. Comput. Math.*, pages 1–33, 2025.

[LS20] Y. Lu and S. Steinerberger. Synchronization of kuramoto oscillators in dense networks. *Nonlinearity*, 33(11):5905, 2020.

[LXB19] Shuyang Ling, Ruitu Xu, and Afonso S Bandeira. On the landscape of synchronization networks: A perspective from nonconvex optimization. *SIAM J. Optim.*, 29(3):1879–1907, 2019.

[McR25] Andrew D. McRae. Benign landscapes for synchronization on spheres via normalized laplacian matrices. Preprint, 2025.

[MLGW24] Takeru Miyato, Sindy Löwe, Andreas Geiger, and Max Welling. Artificial kuramoto oscillatory neurons. Preprint, 2024.

[MMJ87] D. C. Michaels, E. P. Matyas, and J. Jalife. Mechanisms of sinoatrial pacemaker synchronization: a new hypothesis. *Circ. Res.*, 61(5):704–714, 1987.

[MP05] Pablo Monzón and Fernando Paganini. Global considerations on the Kuramoto model of sinusoidally coupled oscillators. In *Proceedings of the 44th IEEE Conference on Decision and Control*, pages 3923–3928. IEEE, 2005.

[MPT05] Yuri L Maistrenko, Oleksandr V Popovych, and Peter A Tass. Chaotic attractor in the kuramoto model. *Internat. J. Bifur. Chaos Appl. Sci. Engrg.*, 15(11):3457–3466, 2005.

[MS06] Alexander S. Mikhailov and Kenneth Showalter. Control of waves, patterns and turbulence in chemical and biological systems. *Phys. Rep.*, 425(2–3):79–194, 2006.

[NM11] A. Nabi and Jeff Moehlis. Single input optimal control for globally coupled neuron networks. *J. Neural Eng.*, 8(6):065008, 2011.

[OS06] Reza Olfati-Saber. Flocking for multi-agent dynamic systems: Algorithms and theory. *IEEE Trans. Automat. Control*, 51(3):401–420, 2006.

[PS89] U. N. Peled and M. K. Srinivasan. The polytope of degree sequences. *Linear Algebra Appl.*, 114:349–377, 1989.

[SS93] Steven H. Strogatz and Ian Stewart. Coupled oscillators and biological synchronization. *Sci. Am.*, 269(6):102–109, 1993.

- [Str00] Steven H. Strogatz. From kuramoto to crawford: exploring the onset of synchronization in populations of coupled oscillators. *Phys. D*, 143(1–4):1–20, 2000.
- [Tay12] Richard Taylor. There is no non-zero stable fixed point for dense networks in the homogeneous kuramoto model. *J. Phys. A: Math. Theor.*, 45(5):055102, 2012.
- [TSS20] Alex Townsend, Michael Stillman, and Steven H. Strogatz. Dense networks that do not synchronize and sparse ones that do. *Chaos*, 30(8):083142, 2020.
- [Win67] Arthur T. Winfree. Biological rhythms and the behavior of populations of coupled oscillators. *J. Theoret. Biol.*, 16(1):15–42, 1967.
- [YTT21] Ryosuke Yoneda, Tsuyoshi Tatsukawa, and Jun-nosuke Teramae. The lower bound of the network connectivity guaranteeing in-phase synchronization. *Chaos*, 31(6):063124, 2021.

ETH ZÜRICH, SWITZERLAND

*Email address:* hongjin-wu@outlook.com

ETH ZÜRICH, SWITZERLAND

*Email address:* ubrandes@ethz.ch